Fast magnetic field penetration into a cylindrical plasma of a nonuniform density

K. Gomberoff and A. Fruchtman
Department of Physics, Weizmann Institute of Science, Rehovot 76100, Israel

(Received 8 January 1993; accepted 3 May 1993)

The penetration of a magnetic field into a cylindrical plasma of a density that varies both radially and axially is studied. The magnetic field penetrates rapidly due to the Hall field, along constant nr^2 lines (n is the dimensionless plasma density and r is the dimensionless radial coordinate). For a plasma that conducts between two cylindrical electrodes, it is shown that there is magnetic field penetration for both positive and negative polarity cases as long as there is penetration along the electrodes. The magnetic field evolution is found, analytically and numerically, for different time behaviors of the magnetic field at the boundaries. Ion velocities are also calculated.

I. INTRODUCTION

Fast magnetic field penetration into a plasma due to the Hall field has been the subject of many recent studies. In particular, it has been shown that the penetration can result from a density gradient in a planar geometry,[1] or from a magnetic field curvature in cylindrical geometry.[2] In order for the fast magnetic field penetration to be the dominant mechanism, plasma pushing by the magnetic field has to be negligible. This occurs when the ion speed is smaller than the field penetration speed (defined later in the text), or equivalently $L < c/\omega_{pi}$ (L is the length scale of the density gradient or the radius of curvature of the magnetic field and c/ω_{pi} is the ion skin depth).[3] On the other hand, if the ion speed is larger than the field penetration speed, or equivalently $L > c/\omega_{pi}$, the plasma pushing is dominant.[4] Both cases, the density gradient case and the cylindrical magnetic field curvature case lead to similar equations for the evolution of the magnetic field, when equivalent parameters are identified. From the assumption of quasineutrality, it is required that $L > c/\omega_{pe}$ (c/ω_{pe} is the electron skin depth). The assumptions of quasineutrality on one hand and negligible ion motion on the other hand require the relevant scale length of the model to satisfy $c/\omega_{pe} < L < c/\omega_{pi}$.

In the previously mentioned cases, the resistivity is assumed small, so that the magnetic field diffusion is much slower than the magnetic field penetration. This is the case when $\eta/\eta_H \ll 1$ (η is the collisional resistivity and $\eta_H = B/N_{ec}$ is the "Hall resistivity," B is the magnetic field, N is the plasma density, $-e$ is the electron charge, and c is the light velocity in vacuum). The magnetic field penetrates in a direction perpendicular to the density gradient in the planar case or in the axial direction (perpendicular to the radial direction) in the cylindrical case. The penetration is in the form of a shock wave, where the shock structure depends on the resistivity. The velocity of propagation and the amount of dissipation, however, do not depend on the resistivity.[5] In addition to the Hall-induced penetration in which the resistivity determines the shock structure,[1-3,5-9] recent studies have treated the penetration in the case in which the resistivity is very small and the electron inertia is dominant.[10-13]

Motivated by the question of the magnetic field penetration into the plasma in the plasma opening switch (POS),[14,15] we concentrate on the cylindrical case. We study the penetration of the magnetic field into a hollow cylindrical plasma that fills the gap between two concentric cylindrical conductors at some axial location. In our previous studies we assumed that the plasma density was uniform. We showed that if the cathode is at the inner conductor (negative polarity), the magnetic field penetrates axially into the plasma from the vacuum. If the cathode is at the outer conductor (positive polarity), there is no field penetration. Moreover, if the plasma is initially magnetized, then the field is spontaneously expelled. In both cases, since the density is uniform, the evolution of the magnetic field near the electrodes does not affect much the evolution of the magnetic field in the bulk of the plasma.[9]

In the present paper, we assume that the (dimensionless) plasma density n is not uniform. The density distribution is assumed to be realistic and to decrease axially toward the vacuum–plasma boundary. We also allow a radial density variation. We show that the magnetic field evolution is along constant nr^2 lines. The uniform density case is therefore only a special case, in which the constant nr^2 lines are parallel to the axial direction. We show that in contrast to the uniform density cylindrical case, in the nonuniform density cylindrical case the magnetic field penetrates for both switch polarities, as long as there is fast magnetic field penetration along the electrodes. This is because the constant nr^2 lines are not parallel to the axial direction, but rather end at the neighborhood of the electrodes. If the penetration along the anode is faster (as in our two-dimensional study[9]), the major penetration of the magnetic field for both polarities occurs from the anode. In a recent paper we have described qualitatively the penetration of the magnetic field into a plasma of a realistic density profile.[16]

We assume that the resistivity is small enough so that the dominant process is the Hall-induced penetration along the nr^2 contour lines. On the other hand, the resistivity is assumed to be not too small, so that the fluid description is still correct and the electron inertia can be neglected. By neglecting the resistive term, we obtain a hyperbolic equation that is solved by calculating its characteristics. The

 0899-8221/93/5(8)/2841/12/$6.00

solutions that we find have shock discontinuities and also discontinuities at the plasma boundaries. Within our model the discontinuities can be removed by adding finite resistivity. In reality, there could be non-neutral sheaths that remove the discontinuities.[17] The nr^2 contour lines are the projections of the characteristics onto the (r,z) plane (z is the dimensionless axial coordinate). Since the nr^2 contour lines intersect the electrodes, the evolution of the magnetic field in the neighborhood of the electrodes is crucial to the evolution in the bulk of the plasma. A correct treatment of the evolution near the electrodes involves an appropriate treatment of the non-neutral sheaths. Elaborate models were developed for that purpose. Common to these models is the prediction of the fast penetration of the magnetic field along the cathode[14,15,17–19] or along the anode.[9,20] Thus, here we assume that the magnetic field does penetrate into the plasma along the electrodes by some mechanism.

We calculate analytically the penetration of the magnetic field for various time behaviors of the magnetic field at the plasma boundaries. First, we consider a magnetic field that is fast rising to a constant value (step function in time). We study the time evolution of the magnetic field and the steady state that is reached. We then study the case in which the magnetic field is linearly rising in time. Finally, a linearly rising magnetic field that is followed by a decreasing magnetic field is considered. Examples are given for both polarities. Numerical results are given for negative polarity and finite resistivity. In addition, we calculate the ion velocities that result from the Hall electric field, for such parameters that the ion displacement is small, consistent with the assumptions of the model. Also, the velocity of the wave propagation is shown to be greater than the Alfvén velocity V_A, satisfying the requirement[3] for the plasma pushing to be negligible. All the examples given in this paper are relevant only for the short conduction time POS.

In Sec. II the model is presented and the evolution along constant nr^2 density lines is shown. In Sec. III the uniform density case and the nonuniform density case are compared briefly. In Sec. IV a realistic density profile is described. Analytical solutions for various time behaviors of the magnetic field at the boundaries are given in Sec. V. In Sec. VI the ion velocities are calculated under the assumption that they are accelerated by an electric field that results mainly from the Hall term. Finally, Sec. VII is dedicated to conclusions. Some calculations are left for an appendix.

II. THE MODEL

We assume that the main process is the fast magnetic field penetration into the plasma due to the Hall field and that the ion motion can be neglected. We also assume that the electron inertia and the displacement current can be neglected, and that the plasma is cold. Elsewhere,[5] the effect of electron heating is studied for a particular case of our model. The equations describing our model are Faraday's law,

$$\nabla\times\mathbf{E}=-\frac{1}{c}\partial_T\mathbf{B},$$

Ampère's law,

$$\nabla\times\mathbf{B}=(4\pi/c)\mathbf{J},$$

and the momentum equation of the electron (Ohm's law),

$$\mathbf{E}=\eta\mathbf{J}+(\mathbf{J}\times\mathbf{B})/eNc,$$

where $\mathbf{E}$ and $\mathbf{B}$ are the electric and magnetic fields and $\mathbf{J}$ is the current density. We also assumed that the scale length of the density gradient and the radius are smaller than c/ω_{pi}, otherwise the main process is plasma pushing by the magnetic field. In this case the ions barely move and $\mathbf{J}=-eN\mathbf{V}_e$ and $\partial_T N=0$ ($\mathbf{V}_e$ is the electron flow velocity). In order to also neglect the electron inertia we assumed that the plasma is collisional enough.

The geometry assumed in our model is that of a POS. A plasma fills a space of axial length a between two concentric cylindrical electrodes. The outer electrode has radius r_o and the inner electrode has radius r_i. A magnetic field is applied in the vacuum on one side of the plasma (the generator side). The magnetic field in the vacuum on the other side of the plasma (the load side) is assumed to remain zero. The magnetic field in the vacuum on the generator side at the inner conductor is B_i. We assume also that $\mathbf{B}=B\hat{\theta}$ and that derivatives with respect to θ are zero. We choose the generator to be in the negative z direction. In that case, for negative polarity $B<0$, while for positive polarity $B>0$.

Under these assumptions, after defining dimensionless parameters:

$$r\equiv\frac{R}{r_i};\quad z\equiv\frac{Z}{a};\quad n\equiv\frac{N}{n_0};\quad b\equiv-\frac{RB}{r_iB_i},$$

$$t\equiv\frac{cB_iT}{4\pi r_i n_0 ea},\quad \eta'\equiv\frac{en_0c\eta}{B_i},$$

we obtain

$$\partial_t b=\frac{\eta' a}{r_i}\left(\frac{r_i^2}{a^2}\partial_z^2 b+r\partial_r\frac{1}{r}\partial_r b\right)-rb\left\{\frac{1}{nr^2},b\right\},\tag{1}$$

where $\{w,l\}=\partial_z w\,\partial_r l-\partial_r w\,\partial_z l$ (Poisson brackets) and n_0 is the maximum density in the plasma. We define new orthogonal coordinates ξ and ω, where

$$\xi\equiv nr^2,\tag{2}$$

and ω is such that $\nabla\xi\cdot\nabla\omega=0$. The last condition together with $d\omega[z(r),r]/dr=(\partial\omega/\partial z)(dz/dr)+\partial\omega/\partial r=0$ define constant ω lines for r and z, satisfying

$$\frac{dz}{dr}=\frac{\partial_r\xi}{\partial_z\xi}.\tag{3}$$

We assume that $\eta' a/r_i\ll 1$; therefore we neglect the first term on the right-hand side of Eq. (1) and we obtain an hyperbolic equation for the magnetic field:

$$\partial_t b=-G(\xi,\omega,b)\partial_\omega b,\tag{4}$$

where $G(\xi,\omega,b)\equiv(b/r^3n^2)\{\xi,\omega\}$. The magnetic field is constant along the characteristic (t,ω_I), with the following equation for the magnetic field and the characteristic:

$$b[t,\omega_I(t),\xi]=b_0\equiv b[t_0,\omega_I(t_0),\xi],$$

$$\frac{d\omega_I}{dt}=G(\xi,\omega_I,b_0). \tag{5}$$

An initial b_0 value at one point of the $nr^2=\xi_0$ curve, and at initial $\omega_0=\omega_I(t_0)$, propagates with the velocity $G(\xi_0,\omega,b_0)$ along the constant ξ_0 curve.

Kulsrud *et al.*[21] have pointed out that since b/nr^2 is constant along an electron trajectory, a steady-state current distribution is usually impossible. Fruchtman[22] has shown that as a result the magnetic field evolves in time, so that b/nr^2 remains constant along the trajectory of the electron. The present analysis shows that the magnetic field evolves along the nr^2 lines [Eq. (5)]. During this evolution the electrons move across the nr^2 contour lines. If a steady state is reached as a result of the evolution, the magnetic field b is constant along nr^2 contour lines and the current and the electron trajectories are parallel to these lines.

The velocity of propagation $G(\xi,\omega,b)$ along the characteristic is proportional to the magnetic field. Reversing the sign of the magnetic field (which corresponds to reversing the polarity in the POS configuration) reverses the direction of propagation along the constant ξ curve.

Knowing that the evolution is along constant ξ lines, let us assume that at one point of the ξ_0 curve $b[t_0,\xi_0,\omega(t_0)]=b_0$ and $\omega_I(t)=\omega[z_I(t),r_I(t)]$, where $n_Ir_I^2=\xi_0$. Neglecting the resistive term in Eq. (1), we find that the propagation of b is along constant nr^2 lines, where the characteristics $z_I(t)$ and $r_I(t)$ satisfy

$$\frac{dz_I}{dt}=-r_Ib_0\partial_r\frac{1}{r^2n}, \tag{6}$$

$$\frac{dr_I}{dt}=r_Ib_0\partial_z\frac{1}{r^2n}, \tag{7}$$

where $n(z_I,r_I)r_I^2=\xi_0$.

Let us now assume that the field $b=b_0$ penetrates in a region, where it has a different value $b=b_-$, so that a discontinuity is formed. The velocity of propagation of the discontinuity can be found by rewriting Eq. (4) as $\partial_tR+\partial_\omega S=0$, where $S=b^2/2$ and $R=b^2/G(\xi,\omega,b)$, and by integrating the new equation with respect to ω in a region that contains the discontinuity.[23] The weak solution conserves the magnetic field flux as it should rather than the magnetic field energy. The equation for the location of the discontinuity is

$$\frac{d\omega_d}{dt}=\frac{(b_0-b_-)}{2}\frac{G(\xi,\omega,b)}{b}. \tag{8}$$

If $b_-=0$, the discontinuity propagates at half the velocity of the magnetic field, not at the discontinuity.

The solution of the hyperbolic equation (4), is fully determined by only part of the physical boundary conditions (at one point of the constant ξ curve). When the complete boundary conditions are specified, the mathematical problem is over determined, and a discontinuity is formed at one of the two ends of the constant ξ curve. As is often the case, the discontinuity is removed by the resistive term. With finite resistivity the equation is not hyperbolic anymore, and allows to specify the boundary conditions on both sides of ξ. The discontinuities are smoothed, permitting continuous transition from one value of b to another. Mathematically, the evolution of the magnetic field is not purely along the nr^2 lines. When the resistive term is included, the shock is continuous and its structure depends on the resistivity. The velocity of the shock propagation is independent of the resistivity, as long as $\eta' a/r_i\ll 1$. Therefore we have neglected the resistive term. The presence of finite resistivity, even if its value is small, is crucial for this shock penetration of the magnetic field. As we mentioned before, in the regions in which the resistivity could be neglected (outside the shock layer), b/nr^2 is constant along the electron trajectories, and the frozen-in law is satisfied. Inside the shock layer, however, the nonzero resistivity is crucial, b/nr^2 is not constant along the electron trajectories, the frozen-in law is not satisfied,[22] and there is a large flux penetration.

III. PENETRATION OF MAGNETIC FIELD INTO UNIFORM AND NONUNIFORM CYLINDRICAL PLASMAS

A. The case of plasma of uniform density

When the density is uniform, the constant nr^2 curves are constant r curves. This case has been solved in detail,[3,5,9] where two-dimensional geometry including conducting electrodes at the boundaries, electron heating, and ion motion have been taken into account. It has been shown there that the evolution at the bulk of the plasma is not affected much by the boundary conditions, and that near the anode (when it is made of a conducting surface) the magnetic field penetration is fast. The magnetic field evolution is very different for the two switch polarities. In the negative polarity case the magnetic field propagates from the vacuum on the generator side toward the load side, in the form of a shock wave of velocity $cB_ir_i/4\pi nr^2e$. The width of the shock was shown to be $cen\eta r^2/B_ir_i$, which should be larger than c/ω_{pe}.[6]

When the polarity is positive, the magnetic field propagates from the load side to the generator side. Therefore, if the plasma is initially unmagnetized, it will remain so. Furthermore, if the plasma is initially magnetized, there will be magnetic field expulsion.[9]

B. The case of plasma of nonuniform density

When the plasma is not uniform, constant nr^2 lines intersect the boundaries of the plasma with the electrodes and not only the boundaries of the plasma with the vacuum. The difference between the magnetic field evolution for the two switch polarities is not as drastic as it is when the plasma is uniform. If there is magnetic field penetration along the electrodes, there is also magnetic field penetration into the plasma. A penetration of the magnetic field along the cathode and the generation of a cathode sheath

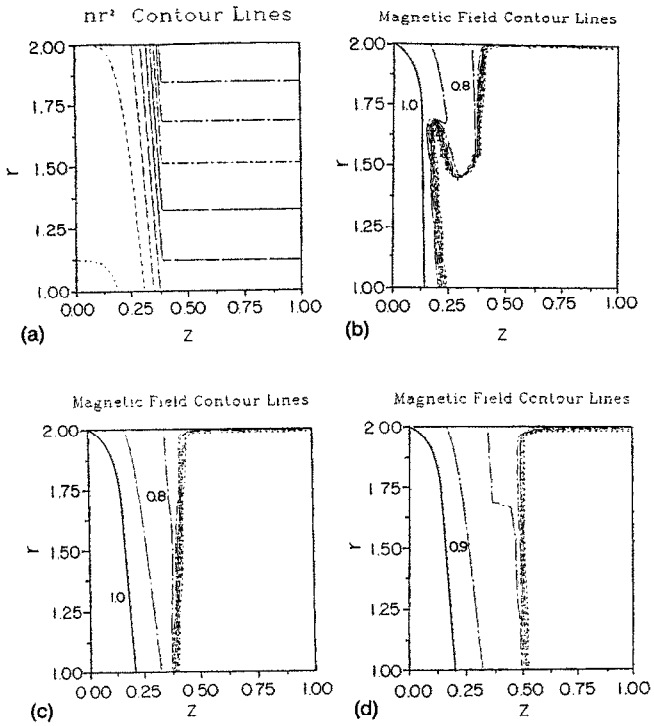

FIG. 1. Numerically calculated magnetic field evolution in a plasma of nonuniform density when the polarity is negative. (a) Contour lines of nr^2: $n=0.1+(2.45z)^5$ for $z<0.4$, $n=1$ for $z>0.4$; (b) contour lines of b, $t=0.2$; (c) $t=0.4$; and (d) $t=0.8$. The magnetic field at the boundaries is a step function in time and $\eta' a/r_i=0.001$. At the cathode, $\partial b=0$.

were shown to be important for the POS operation.[14,15,17–19] There will also be magnetic field penetration along the anode, if the anode is a conductor.[9] We, therefore, assume that the magnetic field penetrates along both electrodes. As we will show here, the magnetic field penetration along the anode is more important for the field penetration into the bulk of the plasma.

In Fig. 1(a), the nr^2 contour lines are shown for a particular density profile. In Figs. 1(b)–1(d), the magnetic field penetration in a negative polarity case is shown for the density profile that is shown in Fig. 1(a). Near the plasma boundary on the left side, where the magnetic field is applied (the generator side), there is a region of a nonuniform density. To the right of that region the plasma density is uniform. A magnetic field $b=1$ is applied at $t=0$ on the left boundary. The magnetic field at the boundary on the right is assumed zero. We assume an infinitely fast penetration of the magnetic field along the anode. At the cathode, on the other hand, the radial derivative of the magnetic field is assumed zero. This is a numerical solution that also includes resistivity. The boundary condition at the cathode makes the resistive solution different from the nonresistive solution that propagates along the constant nr^2 characteristic. Far from the cathode the evolution is along constant nr^2 lines, and the solution becomes the familiar one in the uniform region.

The "S-shaped" structure in Fig. 1(b) is due to the nonmonotonic-in-z radial velocity of the field propagation, which is a result of a nonmonotonic-in-z dependence on $(d/dz)(1/n)$ for the particular density profile of Fig. 1(a). In a realistic density profile at the plasma–vacuum boundary, the dependence is usually monotonic, and the "S-shaped" structure is not expected to appear. However, such a "S-shaped" structure is a true physical phenomenon that could occur in reality whenever a region of nonuniform density exists in the plasma between two regions of a more uniform density.

IV. REALISTIC DENSITY PROFILE

We assume now a realistic density profile of the form

$$n=f(z)r^{\alpha}, \tag{9}$$

where $f(z)$ is assumed to decrease toward the vacuum–plasma boundaries. The density profile in actual experiments depends on the preparation of the plasma. We choose as a particular example a trapezoidlike plasma injection from the cylinder axis, and consequently we assume that $-2<\alpha\leqslant -1$. From Eqs. (2) and (3), we obtain

$$\xi=f(z)r^{\alpha+2},$$

$$\omega=\int \frac{f}{df/dz}\,dz-\frac{r^2}{2(\alpha+2)}.$$

From Eqs. (6) and (7) we find that the propagation along constant ξ is given by

$$\frac{dz_I}{dt}=\frac{b_0(\alpha+2)}{\xi}, \tag{10}$$

$$\frac{dr_I}{dt}=-\frac{b_0(df/dz)}{r_I^{\alpha+1}f^2}. \tag{11}$$

Note that along constants ξ, dz_I/dt is also constant. This is a result of the particular choice of the density radial dependence, and simplifies the calculations considerably. We now assume

$$f(z)=[1+4(\epsilon-1)(z-\tfrac{1}{2})^2]. \tag{12}$$

There is a discontinuity in the density at the vacuum–plasma boundary, when taking $\epsilon\neq 0$, which is only an approximation for the density profile. Also note that $f(z=\frac{1}{2})=1$.

Suppose that at the boundaries (either with the electrodes or with the vacuum) a magnetic field $b=b_0(\xi)$ is specified, which propagates along constant ξ. Equations (10) and (11) are integrated to give

$$z_I(t)=\frac{b_0(\alpha+2)t}{\xi}+z_0, \tag{13a}$$

where for positive polarity,

$$z_0=-\sqrt{\frac{\xi-1}{4(\epsilon-1)}}+0.5, \quad \text{for } z<\frac{1}{2},$$

$$z_0=\sqrt{\frac{\epsilon/r_0^{\alpha+2}-1}{4(\epsilon-1)}}+0.5, \quad \text{for } z>\frac{1}{2}. \tag{13b}$$

For negative polarity the values of z_0 for $z>\frac{1}{2}$ and $z<\frac{1}{2}$ are interchanged. When z_0 becomes greater than unity or less than zero in Eq. (13b), the constant nr^2 lines end at the vacuum–plasma boundaries, and z_0 is unity or zero, respectively. The evolution in time of $r_I(t)$ is

$$r_I(t)=\left(\frac{\xi}{1-[-(2b_0/\xi)\sqrt{1-\epsilon}(\alpha+2)\mathrm{sgn}(\frac{1}{2}-z)t+\nu]^2}\right)^{1/(\alpha+2)}, \tag{14}$$

where for positive polarity,

$$\nu=-\sqrt{1-\xi}, \quad \text{for } z<\tfrac{1}{2},$$

and

$$\nu=\sqrt{1-\xi/r_0^{\alpha+2}}, \quad \text{for } z>\tfrac{1}{2}.$$

Again, for negative polarity the values of ν for $z>\frac{1}{2}$ and $z<\frac{1}{2}$ are interchanged. Equation (14) follows the relation $n[r_I(t),z_I(t)]r_I^2(t)=\xi$.

V. VARIOUS BOUNDARY CONDITIONS

As mentioned in the Introduction, the evolution of the magnetic field near the electrodes requires a separate study. We assume here that the magnetic field penetrates along the electrodes, as suggested by various models. As boundary conditions, we specify the magnetic field at all the plasma boundaries. Moreover, we assume that the field penetration along the electrodes is very fast, and therefore, for simplicity, we take the value of the magnetic field at the electrodes to be the product of two functions; one that is only time dependent and one that is only coordinate dependent.

We examine the evolution of the magnetic field due to various time behaviors of the magnetic field at the boundaries. The magnetic field at the boundaries is assumed to be $b=b_e(t)$ at the generator side, $b=0$ at the load side, $b=b_e(t)(1-z^{c1})$ at the outer electrode, and $b=b_e(t)(1-z^{c2})$ at the inner electrode.

We also assume that the plasma is initially unmagnetized. We define $h(z_0)$ for positive polarity to be

$$h(z_0)=1-z_0^{c1}, \quad z_0>\tfrac{1}{2},$$

$$h(z_0)=1-z_0^{c2}, \quad z_0<\tfrac{1}{2},$$

while for negative polarity, it is defined as

$$h(z_0)=1-z_0^{c1}, \quad z_0<\tfrac{1}{2},$$

$$h(z_0)=1-z_0^{c2} \quad z_0>\tfrac{1}{2}.$$

For all cases, the method used to find the magnetic field evolution is the same. At each point in the plasma region (r,z), the value of $\xi=\xi(r,z)=n(r,z)r^2$ is found, and then, using Eq. (13b), $z_0(\xi)$ is also calculated. For a time t, it is checked whether the wave has reached this point. The value of the magnetic field is calculated by finding the value that the field had at the boundary at a time $\Delta t(r,z,t)$ (to be found), knowing that the field has propagated for a time $t-\Delta t(r,z,t)$, according to Eq. (13a). The equation for $\Delta t(r,z,t)$ becomes

$$[t-\Delta t(r,z,t)]b_e[\Delta t(r,z,t)][h(z_0)]\frac{(\alpha+2)}{\xi}=(z-z_0). \tag{15}$$

On the other hand, the velocity of propagation of the wave front, where a discontinuity exists, is found by equating the propagation of the discontinuity due to a magnetic field at time Δt_f at the boundary [Eq. (8)] and the propagation of a continuous wave with the same magnetic field [Eq. (13a)]. The equation for Δt_f is

$$[t-\Delta t_f(t)]b_e[\Delta t_f(t)]=\frac{1}{2}\int_0^t b_e[\Delta t_f(t')]dt'. \tag{16}$$

The left-hand side of the equation results from the continuous propagation equation [Eq. (13a)]; the right-hand side results from the discontinuity propagation equation [Eq. (8)].

We now analyze several cases. Case A is of a magnetic field that is switched at the plasma boundaries as a step function. The evolution of the magnetic field in the plasma is calculated. Case B is the steady-state magnetic field distribution in the plasma for the magnetic field that was specified on the boundaries in case A. Case C is the magnetic field that rises linearly in time at the plasma boundaries. Case D is of a nonmonotonic behavior of the magnetic field. To enable analytical calculation the magnetic field is assumed first to rise linearly in time and then to decrease linearly in time. The time evolutions of the magnetic field at the boundaries in the various cases is shown in Fig. 2.

A. Magnetic field switched on as a step function in time

In this case $b_e(t)=\pm\Theta(t)$, where Θ is a step function. From here on the upper sign refers to negative polarity while the lower sign refers to positive polarity. The solution for the magnetic field in this case is

$$b^a(z,t,\xi)=\pm\Theta(t)[h(z_0)]\Theta[\pm(z_f^a(t,\xi)-z)]. \tag{17}$$

The wave front $z_f^a(t,\xi)$ propagates as

$$z_f^a(t,\xi)=\frac{h(z_0)(\alpha+2)t}{2\xi}+z_0. \tag{18}$$

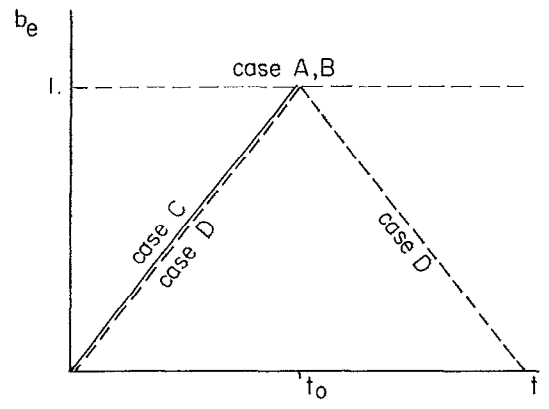

FIG. 2. Illustration of the time behaviors of the magnetic field at the boundaries for cases A–D.

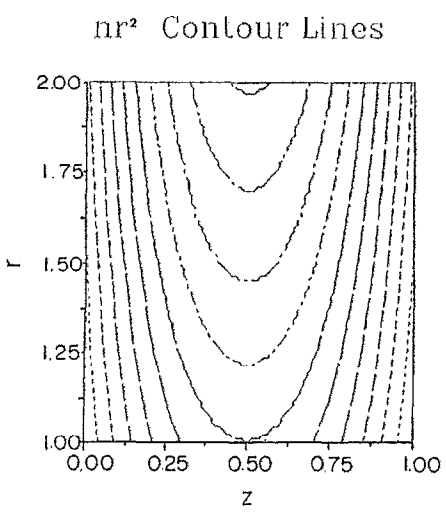

FIG. 3. The nr^2 contour lines of the density profile assumed in all the numerical examples that follow ($\epsilon=0.3$ and $\alpha=-1.5$).

The radial location of the front r_f^a is found from the relation $\xi=n(r_f^a,z_f^a)(r_f^a)^2$. Here $\Delta t_f^a=t/2$.

B. Steady state

We assume that the field is switched on at the boundaries as a stepfunction in time (as in the previous case). After enough time the field in the plasma reaches a steady state. The discontinuities of the magnetic field correspond to infinite current densities and infinite electric fields. Finite resistivity should resolve most of the singularities.

C. Magnetic field linearly rising in time

In this case $b_e(t)=\pm t/t_0$. Let us define $\Delta\tilde{t}\equiv\Delta t/t_0$ and $\tilde{t}\equiv t/t_0$. According to Eq. (15), the magnetic field is

$$b^c(z,t,\xi)=\pm\Delta\tilde{t}\,h(z_0)\Theta[\pm(z_f^c(t,\xi)-z)], \tag{19}$$

where $\Delta\tilde{t}=(\tilde{t}+\sqrt{\tilde{t}^2-4W})/2$, and $W\equiv(z-z_0)\xi/(\alpha+2)t_0[\pm h(z_0)]$ (note that $W>0$).

The velocity of propagation of the front is found from Eq. (16). It is easy to see that the solution for this equation is

$$\begin{aligned}\Delta\tilde{t}_f(\tilde{t})&=\tfrac{3}{4}\tilde{t},\\ b_f^c(\tilde{t})&=\tfrac{3}{4}\tilde{t}[\pm h(z_0)],\\ z_f^c(\tilde{t})&=\tfrac{3}{16}\tilde{t}^2\tilde{t}_0[\pm h(z_0)]\frac{(\alpha+2)}{\xi}+z_0.\end{aligned} \tag{20}$$

Again, r_f^c is found from the requirement $n(r_f^c,z_f^c)(r_f^c)^2=\xi$.

Figure 3 shows the nr^2 contour lines of the density distribution that is used in all the numerical examples that follow. The density parameters are chosen to be $\alpha=-1.5$ and $\epsilon=0.3$.

Figure 4 shows the distribution of the magnetic field, as found analytically by the method described above, at time $t=0.2$, when the polarity is negative. Figure 4(a) shows the distribution when the magnetic field at the plasma boundaries is applied as a step function (case A), while Fig. 4(b) shows the distribution when the magnetic field at the boundaries rises linearly in time (case C), with a rise time $t_0=2$. The maximum value of b in both cases is the same.

D. Magnetic field linearly decaying in time after a linear rise time

In this section we study the magnetic field evolution in a plasma in which the magnetic field at the boundaries is nonmonotonic in time, first it rises, and then decreases. We show that during the decrease of the current interesting physical processes occur, such as reversal of the current direction in certain regions in the plasma, followed by ion deceleration in those regions. Although this time at which the current decreases is of less interest for the operation of the POS, understanding of the processes that occur at this time could help the understanding of the processes that occur during the previous time during which the current rises. In fact, in a recent POS experiment at the Weizmann Institute there were indications that ions decelerate during the current decrease.[24] Our calculations propose that the

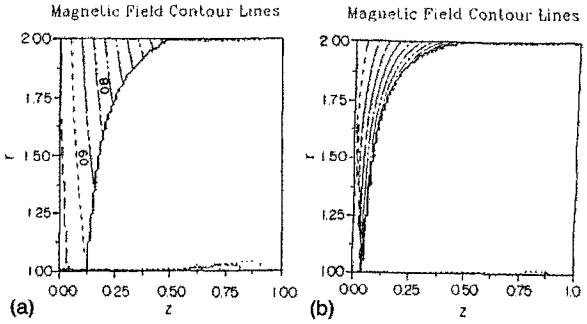

FIG. 4. Analytically calculated magnetic field evolution in a nonuniform plasma (the density profile shown in Fig. 3), for negative polarity at $t=0.2$. The magnetic field at the boundaries ($c_1=c_2=1$) is (a) a step function in time (case A); and (b) rising linearly in time (case C, $t_0=2$).

magnetic field penetration could cause such deceleration. A more quantitative comparison with the experiment will be made in the future, when the measurements are completed.

We choose a time behavior of the magnetic field at the plasma boundaries that only approximates a realistic behavior, but enables us an analytic calculation. We assume that the field rises linearly and reaches a maximum value at $t=t_0$, after which it decreases linearly. The evolution of the magnetic field at the electrodes is therefore assumed to be

$$b_e(\tilde{t})=\pm\tilde{t}, \quad \tilde{t}<1,$$

$$b_e(\tilde{t})=\pm[1-\mu(\tilde{t}-1)], \quad \tilde{t}>1.$$

We refer only to times at which the magnetic field is positive.

For $1<t<\frac{4}{3}$, in the region where $\Delta\tilde{t}$ (as calculated in the case of linearly rising magnetic field) is larger than 1, or for $t>\frac{4}{3}$ in all the plasma, the linearly decreasing b at the electrodes determines the evolution of the magnetic field. Following the same steps as in the previous case (C), we obtain

$$\Delta\tilde{t}^d=\frac{1/\mu+1+\tilde{t}+\sqrt{(1/\mu+1+\tilde{t})^2-(4/\mu)[-W+\tilde{t}(1+\mu)]}}{2}. \tag{21}$$

Note that case C is recovered when $\mu=-1$. The magnetic field is

$$b^d(z,\tilde{t},\xi)=\pm h(z_0)[1-\mu(\Delta t^d-1)]\theta[\mp(z_f^d(\tilde{t},\xi)-z)]. \tag{22}$$

For $\tilde{t}>\frac{4}{3}$ the solution for Δt_f is no longer Δt_f^c. The equation for the front propagation becomes

$$[\tilde{t}-\Delta\tilde{t}_f^d(\tilde{t})][1-\mu(\Delta\tilde{t}_f^d(\tilde{t})-1]$$
$$=\frac{1}{2}\int_{4/3}^{\tilde{t}}[1-\mu[\Delta\tilde{t}_f^d(\tilde{t}')-1]d\tilde{t}'. \tag{23}$$

The solution for $\Delta\tilde{t}^d(t)$ is given in the Appendix. The wave front propagates as

$$z_f^d(\tilde{t})=[\tilde{t}-\Delta\tilde{t}_f^d(\tilde{t})][1-\mu(\Delta\tilde{t}_f^d(\tilde{t})-1)]h(z_0)\frac{(\alpha+2)}{\xi},$$
$$\tilde{t}>\frac{4}{3}. \tag{24}$$

Figures 5 and 6 show the magnetic field evolution when the polarity is positive. Figure 5 shows the magnetic field distribution when a steady state is reached (case B). The arrows show the direction of the electron flow. Figures 6(a) and 6(b) show the magnetic field distribution at $t=0.666$ and at $t=\frac{3}{2}\cdot 0.666$, respectively, when the magnetic field is applied at the boundaries as a step function. Figures 6(c) and 6(d) show the distributions for the linearly increasing in time magnetic field (case C) for $\tilde{t}=1$, and for the nonmonotonic-in-time magnetic field at the boundaries (case D) for $\tilde{t}=\frac{3}{2}$, where $t_0=0.666$, respectively. These times are the same times as in Figs. 6(a) and 6(b) (at $\tilde{t}=1$, case C and case D are identical). As expected, the fastest penetration is in the step function case (A). We also see that the gradient of the magnetic field is nonmonotonic in space. Therefore, there also exist regions where the direction of the electron flow is from the anode to the cathode. Such regions can appear because of the nr^2 configuration (case C), but also when the applied magnetic field decreases (case D). As is shown in the next section, in such regions the force that is exerted on the ions is toward the generator. Ions that are being pushed toward the load would slow down and might even be pushed toward the generator.

VI. ION MOTION

In our model we have assumed that the plasma pushing is negligible. In this section we calculate the ion velocities and displacements that result from the field evolution calculated in our model. If these velocities and displacements are indeed negligible, it justifies *a posteriori* our initial assumption.

We assume that the ions are accelerated due to an electric field $\mathbf{E}=(\mathbf{J}\times\mathbf{B})/enc$, and that their displacement

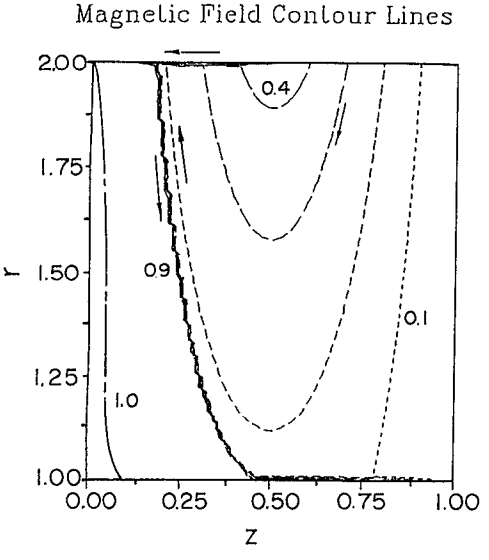

FIG. 5. The steady-state magnetic field distribution in a nonuniform plasma (the density profile is shown in Fig. 3) for positive polarity (case B, $c_2=3$; and $c_1=1$).

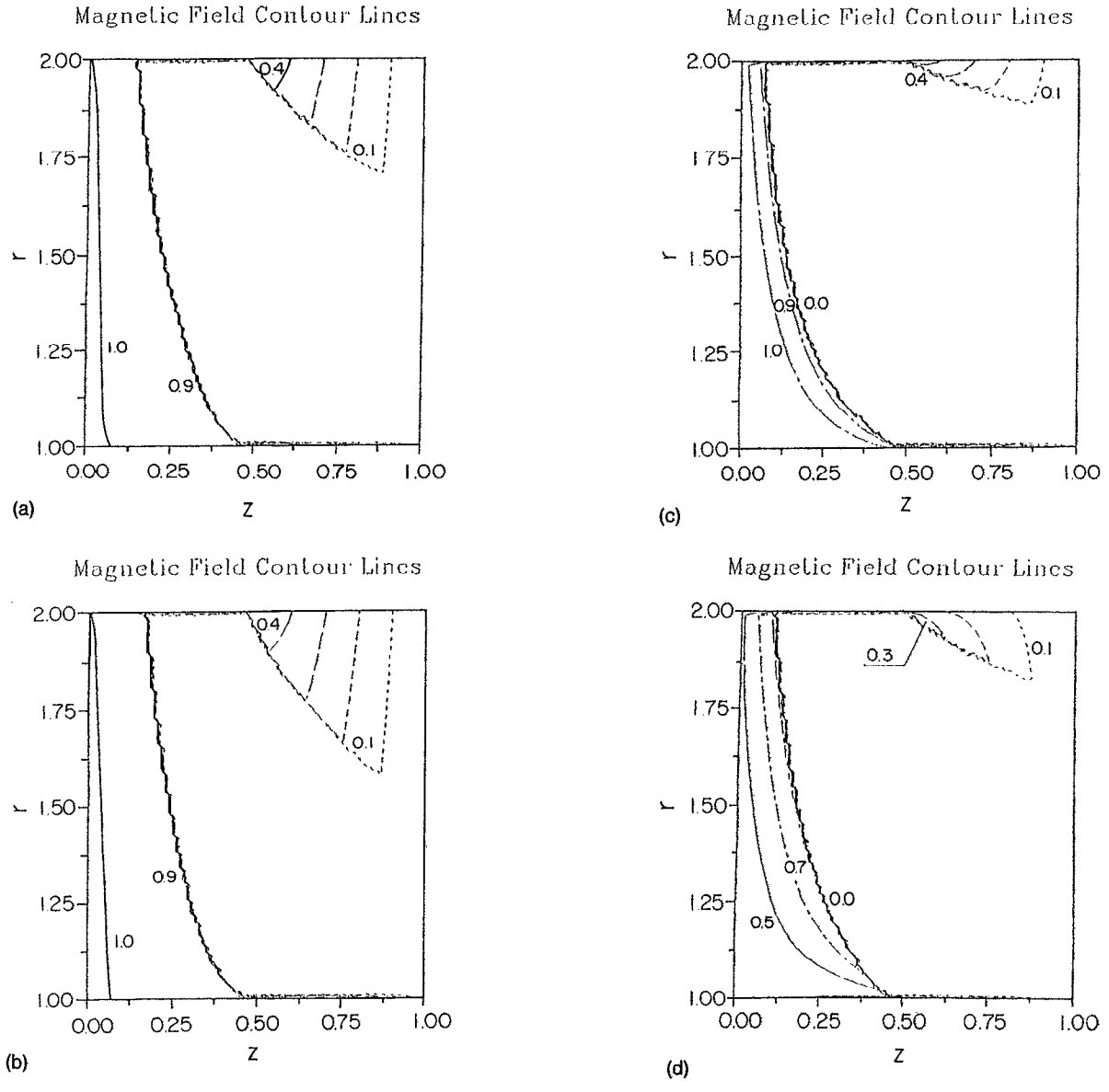

FIG. 6. Magnetic field evolution in a nonuniform plasma (the density profile shown in Fig. 3) for positive polarity. The magnetic field at the boundaries ($c_1=1$, $c_2=3$) is (a) a step function in time (case A) at $t=0.666$, (b) at $t=\frac{3}{2}\cdot 0.666$, (c) is rising linearly in time (case C, $t_0=0.666$) at $t=0.666$, and (d) nonmonotonic in time (case D, $t_0=0.666$, $\mu=1$) at $t=\frac{3}{2}\cdot 0.666$.

is negligible. In terms of dimensionless variables we obtain

$$\frac{d^2 z_{\text{ion}}}{dt} = -\frac{4\pi e^2 r_i^2 n_0}{c^2 M_i}\frac{b\,\partial_z b}{nr^2}, \tag{25}$$

$$\frac{d^2 r_{\text{ion}}}{dt} = -\frac{4\pi e^2 r_i a n_0}{c^2 M_i}\frac{b\,\partial_r b}{nr^2}, \tag{26}$$

where z_{ion} and r_{ion} are the ion axial and radial displacements and M_i is the ion mass. The velocities acquired by the ions result from two kinds of electric fields. The first kind of electric field is a slowly varying weak electric field that exists behind the front, where the current density is low. This electric field exerts force on the ions for a long period of time. The second kind of electric field is the strong electric field at the shock front. This electric field exerts a strong force on the ions, but for a short period of time only, because of the fast propagation.

The ion velocity and displacement due to the weak electric field are found by solving numerically Eqs. (27) and (28). The right-hand sides of the equations are calculated using the values of the magnetic field that were found in the previous sections. In all the calculations we assume that the ion motions are small, so that we approximate the electric fields that the ions experience by the electric fields in their initial positions.

We cannot calculate the ion velocities and displacements that result from the electric fields inside the shock by solving Eqs. (27) and (28), because in our solutions the shocks appear as discontinuities of the magnetic field. The

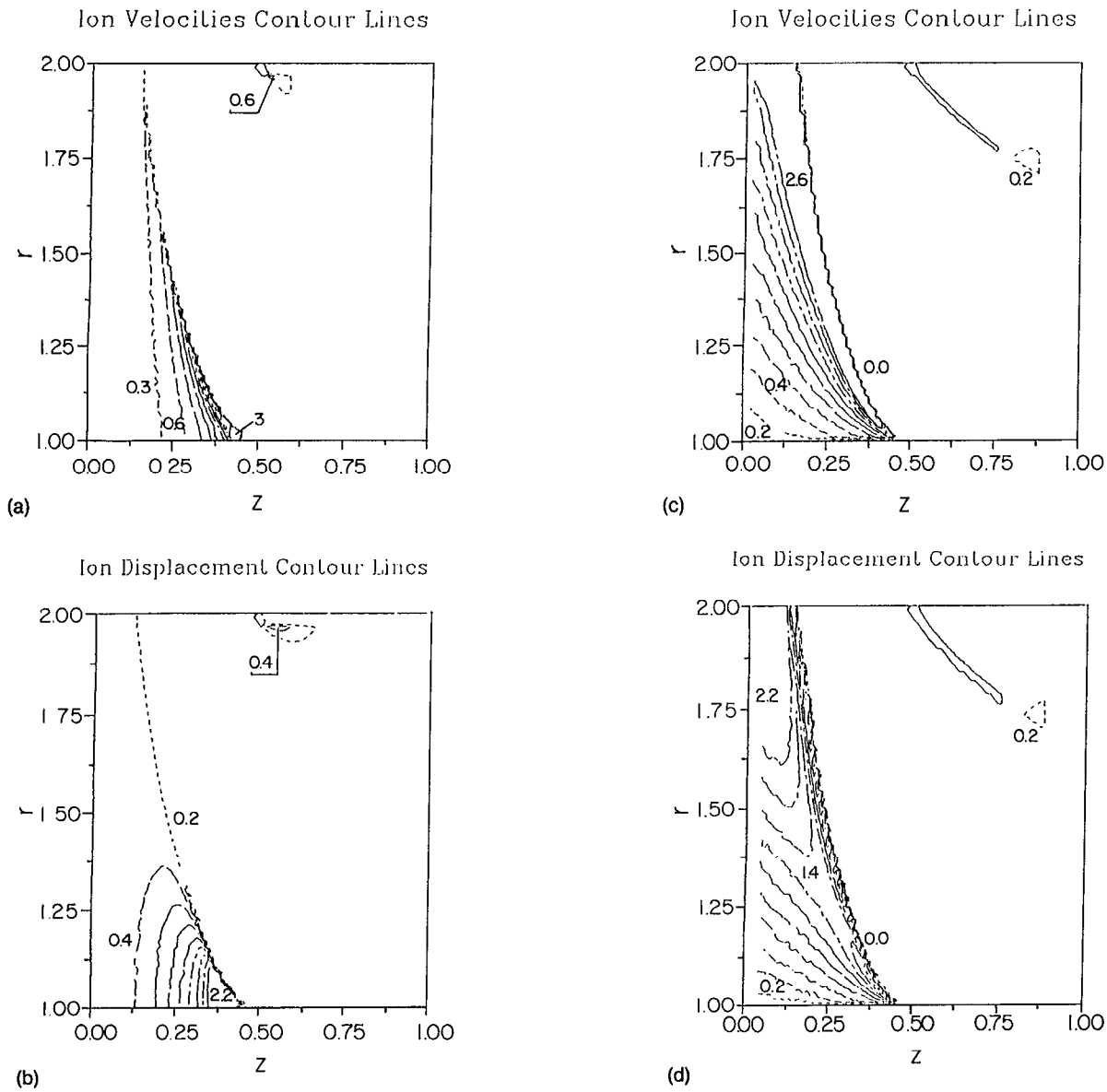

FIG. 7. Ion velocities and displacements that result from the magnetic field evolution shown in Fig. 6(a) (case A), at $t=0.666$ ($\tilde{t}=1$). The parameters are $B_i=10$ kG, $n_0=10^{14}$ cm^{-3}, $M_i=12M_p$ (M_p is proton mass) $a=6$ cm, $r_i=2.5$ cm, $r_o=5.0$ cm, and $T=20$ nsec. (a) $V_{\text{ion},r}$, (b) r_{ion}, (c) $V_{\text{ion},z}$, and (d) z_{ion}. Velocities are in units of 10^7 cm/sec, r_{ion} is in units of $4\times10^{-2}r_i$, and z_{ion} is in units of 2×10^{-2} a.

velocities acquired inside the shock can be estimated by assuming that the time δ that an ion spends inside the shock is so short that the shock velocity V_c can be considered constant. In the rest frame of the shock the ion climbs an electrostatic potential $B^2/8\pi ne$, and acquires the velocity $V_{\text{ion},f}\simeq V_A^2/2V_c$, where $V_A\equiv(B^2/4\pi nM_i)^{1/2}$, and it is assumed that $V_A\ll V_c$. The quantities here are in cgs units. The ion displacement, during the time that an ion spends inside the shock, is of the order of V_{ion}, $f\delta/3$, which is negligible.

In Figs. 7–9 the ion motion that results from the magnetic field evolution in a positive polarity POS is shown. The density profile is shown in Fig. 3 and the calculations are made for the various cases presented in Fig. 6. We chose positive polarity for the numerical example, since in this case the field penetration is smaller than in the negative polarity, and therefore the ion motion is expected to be larger. The main observation is that the plasma ions (which are assumed singly charged carbon ions) acquire only small velocities during the 20 or 30 nsec of field evolution, and that their displacements are small relative to the plasma dimensions. This result justifies *a posteriori* our assumption that the ion motion is negligible.

The ion motion is not negligible in certain regions in the plasma, where large quasistationary gradients of the magnetic field may cause large plasma pushing. Examples are the ion radial displacements at $z=0.5$ near the anode [Figs. 7(b) and 8(b)], and the ion axial displacement at $z=0$ near the cathode [Fig. 8(c)]. Our model is not valid in these regions.

The figures show the ion motion at 20 and 30 nsec. Later, the magnetic field evolution is slower and the ion

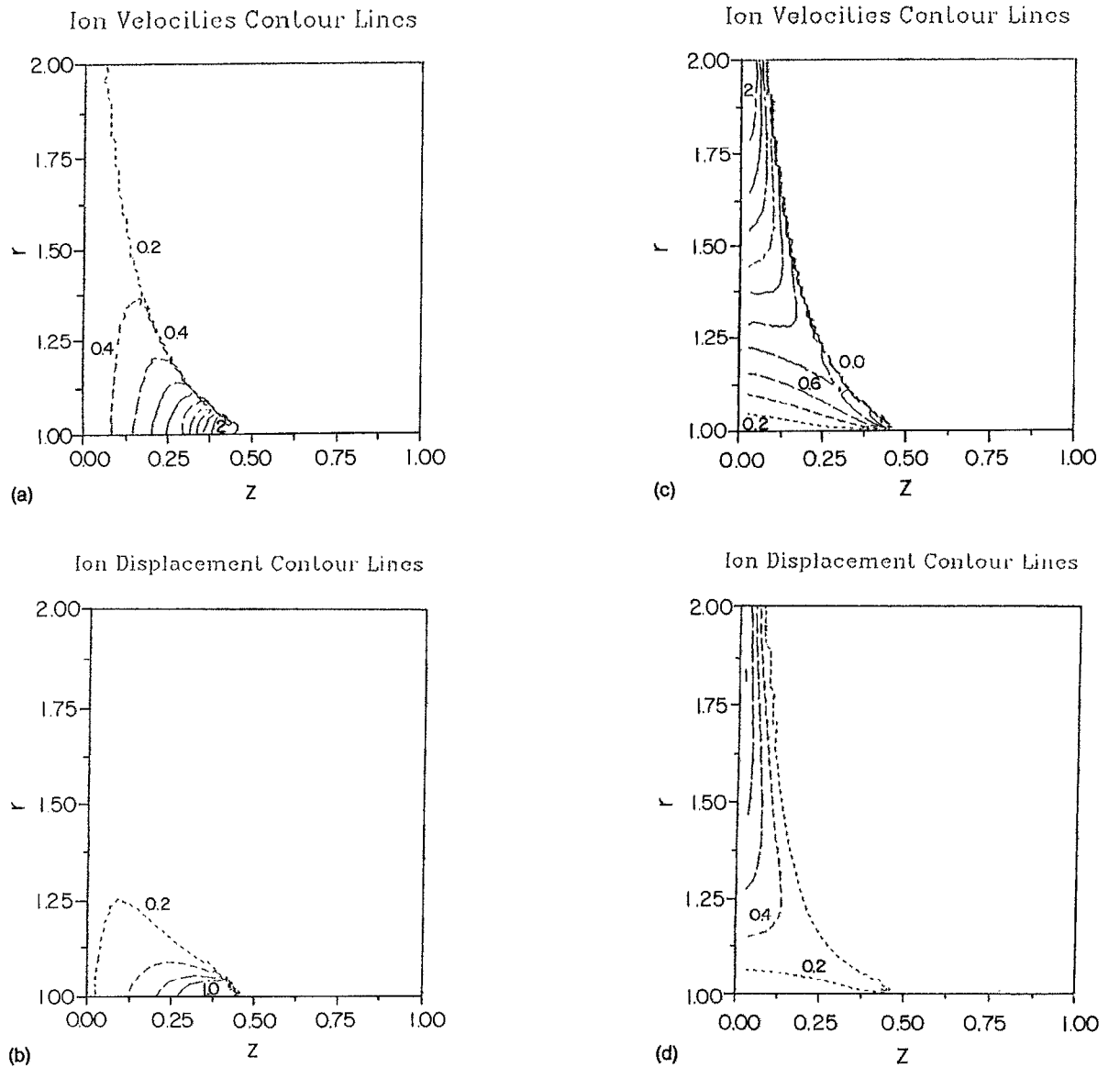

FIG. 8. Ion velocities and displacements that result from the magnetic field evolution shown in Fig. 6(c) (case C), at $t=0.666$ ($\tilde{t}=1$). Here $B_i=10$ kG, $n_0=10^{14}$ cm^{-3}, $M_i=12M_p$ (M_p is proton mass), $a=6$ cm, $r_i=2.5$ cm, $r_o=5.0$ cm, and $T=20$ nsec. The units of velocity and displacement are as in Fig. 7. (a) $V_{\text{ion},r}$, (b) r_{ion}, (c) $V_{\text{ion},z}$, and (d) z_{ion}.

motion becomes more significant. Our calculations show therefore that even in a positive polarity POS, there is a substantial period of time (a few tens of nsec), in which the dominant process is the field penetration.

We also observe that there are regions in the plasma where the ion velocities decrease during the decrease of the magnetic field at the boundaries. Figure 8(a) shows the ion radial velocities at $T=20$ nsec, the time at which the field at the boundaries reaches its maximum. Figure 9(b) shows the radial velocities at $T=30$ nsec, when the magnetic field at the boundaries decreases. It is seen in the figures that the velocities near the anode are smaller at the later time. This is a result of the nonmonotonic-in-space magnetic field [see Fig. 6(d)], and of the electric fields that point toward the anode. The ions are decelerated in those regions.

VII. CONCLUSIONS

In this paper we studied the magnetic field penetration into a plasma in the POS configuration. We have shown that while in a cylindrical plasma of a uniform density the magnetic field penetrates in negative polarity only, in a cylindrical plasma of a realistic nonuniform density the penetration occurs in positive polarity as well, as long as there is magnetic field penetration along the electrodes. This is because when the density is nonuniform, the nr^2 contour lines, along which the magnetic field propagates, intersect the electrodes. In the numerical examples, we have shown that even in a positive polarity POS, there is a substantial period of time (a few tens of nsec for the parameters that we chose), during which the dominant pro-

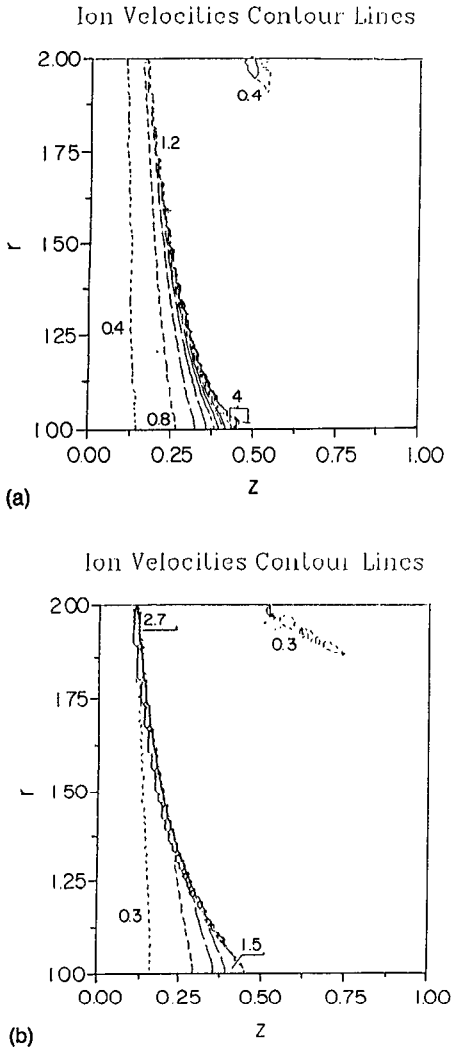

FIG. 9. Ion radial velocities at $\tilde{t}=\frac{3}{2}$ (t_0=0.666) that result from the magnetic field evolution shown in (a) Fig. 6(b) (case A), (b) Fig. 6(d) (case D, $\mu=1$), $B_i=10$ kG, $n_0=10^{14}$ cm^{-3}, $M_i=12M_p$ (M_p is proton mass), $a=6$ cm, $r_i=2.5$ cm, $r_0=5.0$ cm, and the units of velocity are as in Fig. 7. The time is $T=30$ nsec.

cess is the field penetration, and the ion motion is small. Contrary to the negative polarity, however, in the positive polarity the magnetic field usually penetrates into the plasma on the generator side only, and is not expected to reach the plasma boundary on the load side. Thus, in a positive polarity POS, after the initial phase of field penetration, a second phase of plasma pushing by the magnetic field may exist, prior to a power delivery to the load.

Our model is based on several approximations. A more accurate model that treats the non-neutral sheaths near the electrodes[17] and the mutual effects of field penetration and electron heating[5] may modify the results. In addition, as has been recently demonstrated, ion motion may also induce field penetration.[13]

APPENDIX: SHOCK FRONT PROPAGATION FOR CASE D

The solution for the front propagation of case D is as follows. By differentiating Eq. (23), we obtain

$$\frac{d\Delta\tilde{t}_f^d(\tilde{t})}{d\tilde{t}}=-\frac{1}{2}\left(\frac{1+\mu-\mu\,\Delta\tilde{t}_f^d(\tilde{t})}{2\mu\,\Delta\tilde{t}_f^d(\tilde{t})-\mu\tilde{t}-(1+\mu)}\right).$$

We exclude the case $\mu=0$, for which the last equation has the solution $\Delta t_f^d(\tilde{t})=\tilde{t}/2+\frac{1}{3}$ (this is the case of a constant-in-time value of b at the boundary, after a linear rise in time). Defining

$$g\equiv\Delta\tilde{t}_f+a,\quad w\equiv\tilde{t}+\tilde{b},\quad \text{and } p\equiv g/w,$$
$$\text{where } a=-(1+\mu)/\mu;\quad \tilde{b}=-(1+\mu)/\mu,$$

we obtain

$$w\frac{\partial p}{\partial w}=\frac{(-p+\frac{3}{4})\,2p}{2p-1}.$$

This equation has a special solution, $\Delta\tilde{t}_f^d(\tilde{t})=\frac{3}{4}$ for $\mu=-1$ (recovering case C). Otherwise, it leads to a cubic equation for $p\equiv\{\Delta\tilde{t}_f^d(\tilde{t})-[(1+\mu)/\mu]\}/(\tilde{t}-(1+\mu)/\mu)$:

$$(p^3-\tfrac{3}{4}p^2)=(\gamma/w)^3.$$

From the requirement that $\Delta\tilde{t}(\frac{4}{3})=1$, it follows that $\gamma=-(1/4^{1/3}\mu)(1+\mu)^{1/3}$. Defining $\tilde{a}\equiv-(\gamma/w)^3$, we find that p has only one real root $\chi(\tilde{t})=S_++S_-+\frac{1}{4}$, where $S_\pm=\sqrt[3]{-\tilde{a}/2+1/4^3\pm\sqrt{\tilde{a}^2/4-\tilde{a}/4^3}}$. Finally, we obtain

$$\Delta\tilde{t}_f^d(\tilde{t})=\chi(\tilde{t})\left(\tilde{t}-\frac{1+\mu}{\mu}\right)+\frac{1+\mu}{\mu}.$$

[1] A. S. Kingsep, Yu. V. Mokhov, and K. V. Chukbar, Sov. J. Plasma Phys. **10**, 495 (1984).
[2] A. Fruchtman, Phys. Fluids B **3**, 1908 (1991).
[3] A. Fruchtman, Phys. Fluids B **4**, 885 (1992).
[4] C. W. Mendel, Jr., Phys. Rev. A **27**, 3258 (1983).
[5] A. Fruchtman and K. Gomberoff, Phys. Fluids B **4**, 117 (1992).
[6] Ya. L. Kalda and A. S. Kingsep, Sov. J. Plasma Phys. **15**, 508 (1989).
[7] C. R. Devore, J. M. Grossmann, and P. F. Ottinger, Bull. Am. Phys. Soc. **37**, 1564 (1992).
[8] R. J. Mason and P. L. Auer, Bull. Am. Phys. Soc. **37**, 1564 (1992).
[9] A. Fruchtman, Phys. Rev. A **45**, 3938 (1992).
[10] L. I. Rudakov, C. E. Seyler, and R. N. Sudan, Comments Plasma Phys. Controlled Fusion **14**, 171 (1991).
[11] B. V. Oliver, L. I. Rudakov, R. J. Mason, and P. L. Auer, Phys. Fluids B **4**, 294 (1992).
[12] C. E. Seyler, Phys. Fluids B **3**, 2449 (1991).
[13] A. Fruchtman and L. I. Rudakov, Phys. Rev. Lett. **69**, 2070 (1992).
[14] C. W. Mendel, Jr. and S. A. Goldstein, J. Appl. Phys. **48**, 1004 (1977).
[15] B. V. Weber, R. J. Commisso, R. A. Meger, J. M. Neri, W. F. Oliphant, and P. F. Ottinger, Appl. Phys. Lett. **45**, 1043 (1984).
[16] A. Fruchtman and K. Gomberoff, Phys. Fluids B **5**, 2371 (1993).
[17] P. F. Ottinger, S. A. Goldstein, and R. A. Meger, J. Appl. Phys. **56**, 774 (1984).
[18] C. W. Mendel, Jr. (private communication, 1989).
[19] C. K. Ng and R. N. Sudan, J. Appl. Phys. **69**, 137 (1991).
[20] R. J. Mason, M. E. Jones, J. M. Grossmann, and P. F. Ottinger, Phys. Rev. Lett. **61**, 1835 (1988).
[21] R. Kulsrud, P. F. Ottinger, and J. M. Grossman, Phys. Fluids **31**, 1741 (1988).
[22] A. Fruchtman, Phys. Fluids B **4**, 3446 (1992).
[23] F. John, *Partial Differential Equations* (Springer-Verlag, New York, 1971), p. 18.

[24]See National Technical Information Service Document No. PB92-206168 (M. Sarfaty, Ya. Krasik, R. Arad, A. Weingarten, Y. Maron, and A. Fisher, *Spectroscopic investigations of plasma opening switch using a novel gaseous plasma source*, Proceedings of the 9th International Conference on High Power Particle Beams, Washington, DC, 1992, edited by D. Mosher, G. Cooperstein, and V. Granatstein, Washington DC, 25–29 May 1992). Copies may be ordered from the National Technical Information Service, Springfield, Virginia, 22161.